European Conference on Optical Communication (ECOC) 2022 ©
Optica Publishing Group 2022

Compact, Spatial-mode-interaction-free, Ultralow-loss, Nonlinear photonic integrated circuits

Xinru Ji[(1)], Junqiu Liu[(1)], Jijun He[(1)], Rui Ning Wang[(1)],
Zheru Qiu[(1)], Johann Riemensberger[(1)] and Tobias J. Kippenberg[(1)]

[(1)] Institute of Physics, Swiss Federal Institute of Technology Lausanne (EPFL), CH-1015 Lausanne, Switzerland, liujq@iqasz.cn, tobias,kippenberg@epfl.ch

Abstract *We implement Euler bends to build compact high-Q Si_3N_4 racetrack microresonators, featuring a small footprint of only 0.21 mm^2 for 19.8 GHz FSR. We demonstrate that these multi-mode microresonators can be operated in the single-mode regime and generate a single soliton microcomb.*

Introduction

For Kerr nonlinear photonics, anomalous GVD is required, which is realized via geometric dispersion engineering using multi-mode waveguides. However, uncontrollable spatial mode coupling in highly over-moded waveguides is undesired, as it yields spectrally distributed avoided mode crossings (AMXs) with random strengths, prohibiting soliton formation [1] and significantly distorting soliton spectra [2].

Microring resonators are used to avoid mode mixing. Single solitons with repetition rates in the microwave X- and K-band are generated [3], however the devices suffer from significant footprints and constrained device density. Alternatively, mode filtering elements [5] can be used to suppress mode mixing, yet at the same time limit the Q-factor.

Here, we adapt, optimize, and implement Euler bends to build compact racetrack microresonators based on ultralow-loss, multimode, Si_3N_4 photonic circuits. The optimized racetrack microresonators has a significantly reduced device footprint, which is critical for high device density and integration. It can serve as building blocks for nonlinear photonic applications, such as microwave-repetition-rate soliton microcombs, travelling-wave optical parametric amplifiers, frequency conversion, or resonant electro-optic modulators and frequency combs. The adiabatic Euler bend is also useful for linear circuits based on beam splitters and interferometers that are widely used in integrated programmable processors and photonic quantum computing.

Design and simulation

We demonstrate single mode operation in multi-mode Si_3N_4 racetrack microresonators with two symmetric Euler π-bends [6, 7], which have a curvature (k, the inverse of radius) varying linearly with its path length (s), i.e. k(s) = $\alpha \cdot$ s. Partial Euler π-bends, which contain a circular section joint by two symmetric Euler bends, as well as pure circular bends are also used in racetrack microresonators. The portion of Euler bend in a total π-bend is defined with parameter p, such that $p = 1 - \frac{\theta}{\pi}$. A comparison of these three bends are shown in Fig.1(a). Finite-

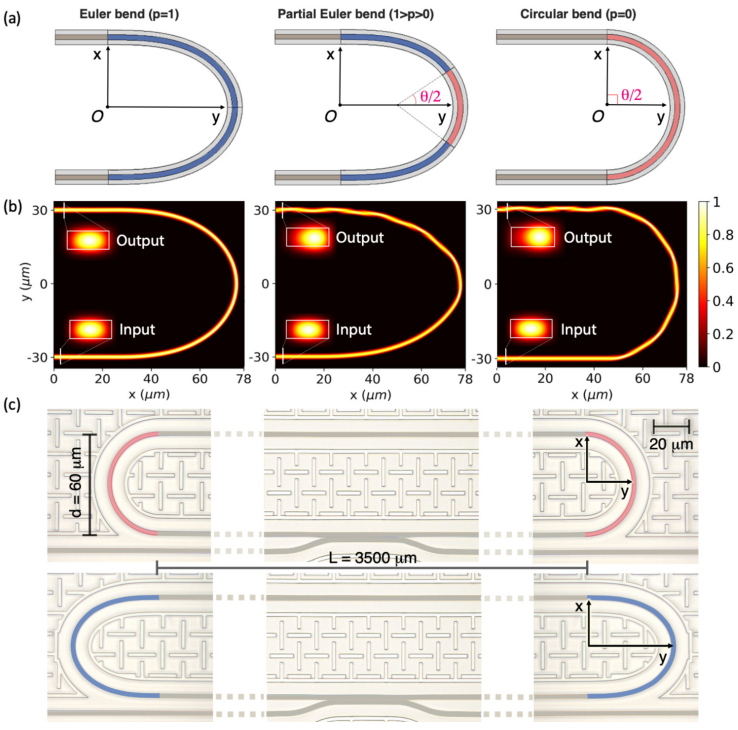

Fig. 1: (a) Schematics of Euler bend, Partial Euler bend and circular bend in Cartesian coordinates x-y. The Euler portion p is defined as $p = 1\text{-}\frac{\theta}{\pi}$; **(b)** Finite-difference time domain (FDTD) simulations of TE00 mode propagation in three bends; **(c)**Optical microscope images showing fabricated Si3N4 racetrack microresonators with Euler bends and circular bends.

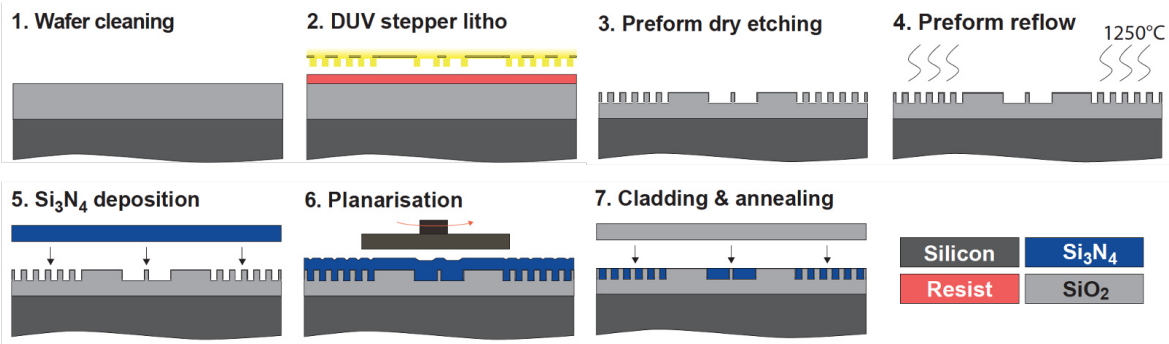

Fig. 2: Photonic Damascene fabrication process for ultra-high *Q* Si_3N_4 microresonators.

difference time domain (FDTD) simulations of mode propagation in these three bends are shown in Fig.1(b). It is observed that the launched TE00 mode is preserved in the Euler bend (p = 1), while it experiences distortion in the partial Euler bend (p = 0.6) and circular bend (p = 0).

Fabrication

The Si_3N_4 integrated devices are fabricated using the photonic Damascene process [8]. Waveguide patterns, as well as filler patterns to release the tensile film stress of Si_3N_4, are exposed with a KrF (248 nm) deep-ultraviolet (DUV) stepper lithography. The patterns are then transferred from the photoresist mask to the thermal wet SiO_2 substrate using dry etching, to create waveguide preforms. A thermal reflow step, where the wafer is annealed at 1250 °C, is performed to reduce the sidewall roughness of waveguide preforms. A Si_3N_4 film of thickness more than 1000 nm is then deposited on the patterned wafer via low-pressure chemical vapour deposition (LPCVD), filling the trenches and forming the waveguides. Chemical-mechanical polishing (CMP) is then used to remove the excess Si_3N_4 and planarize the wafer top surface. Finally, top SiO_2 cladding is deposited on the wafer, followed by high-temperature annealing. The entire wafer is then separated into chips for experiments. The simplified process flow is shown in Fig.2.

The racetrack microresonators consist of two straight waveguides measuring L = 3500 μm in length, and two π-bends spanning d = 60 μm. The microscopic images of fabricated devices are shown in Fig.1(c) The resulted footprint is only 0.21 mm^2 for 19.8 GHz free spectral range (FSR), which is considerably smaller than the footprint of microring resonators of the same FSR that cover an area of more than 4 mm^2 in Ref. [3]. Such a size reduction allows for the integration of 30 devices on a 5 × 5 mm^2 chip. It also benefits devices that have capacitance dependence on area, e.g, piezoelectric modulators [4], where a small footprint allows to reduce the time constant and increase the modulation speed.

Linear measurement

To characterize the resonance linewidths (i. e. microresonator loss) of the fabricated devices, we use frequency-comb-assisted, cascaded diode laser spectroscopy, to cover the entire telecommunication E- to L-band (1350 to 1630 nm) [9]. The intrinsic loss $\kappa_0/2\pi$ and bus-

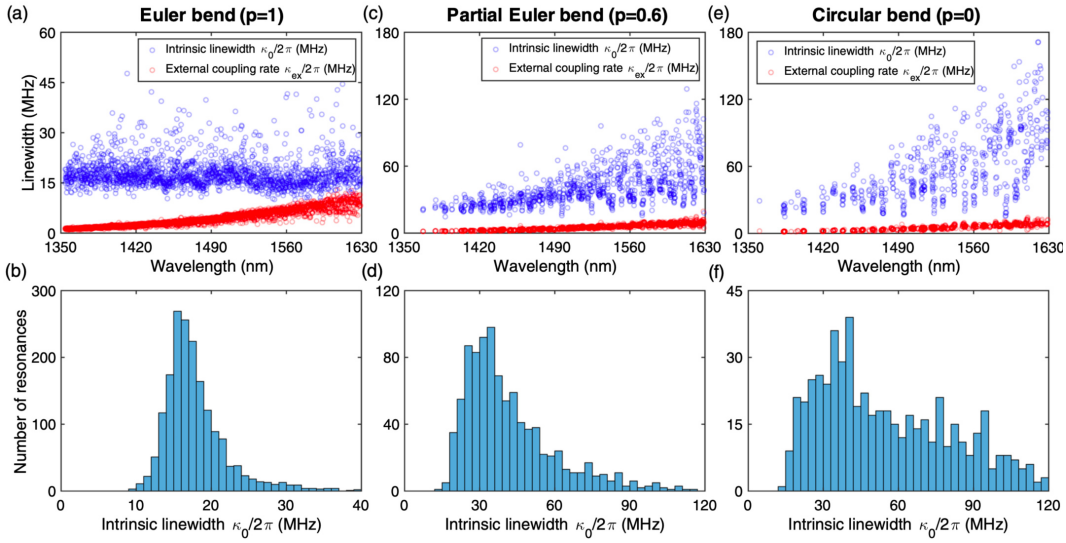

Fig. 3 Resonance linewidth characterization of racetrack microresonators with different bends. Racetrack microresonators with Euler bends (Euler portion p = 1) (a, b), partial Euler bends (p = 0.6) (c, d), and circular bends (p = 0) (e, f) are experimentally characterized. The data shown in (a, c, e) are measured intrinsic linewidth $\kappa 0/2\pi$ and external coupling rate $\kappa ex/2\pi$ over a broad wavelength range for each sample. The data shown in (b, d, f) are histogram of $\kappa 0/2\pi$ from (a, c, e) for each sample.

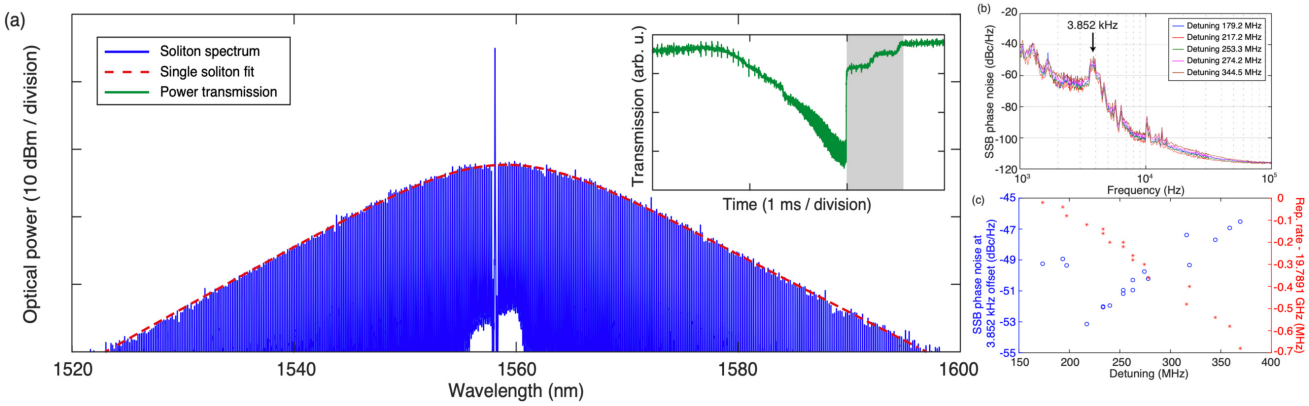

Fig. 4 . Single soliton generation in the racetrack microresonator with Euler bends, and the phase noise characterization of soliton repetition rate. (a) Single soliton spectra of 19.8 GHz repetition rate. No prominent dispersive wave features caused by AMXs are observed. (b) SSB phase noise measurement with different soliton detuning values. (c) SSB phase noise at 3.852 kHz Fourier offset frequency and measured repetition rate shift with different soliton detuning values.

waveguide-to-microresonator external coupling strength $\kappa_{ex}/2\pi$, are given in Fig.3.

For the racetrack microresonator with Euler bends (p = 1) shown in Fig. 3(a, b), no prominent wavelength dependence of $\kappa_0/2\pi$ is observed, and the most probable value in the histogram is $\kappa_0/2\pi$ = 15.5 MHz, corresponding to 2.4 $\mathrm{dB\,m^{-1}}$ linear loss and a microresonator intrinsic quality factor $Q \sim 13 \times 10^6$. However, for the racetrack microresonator with partial Euler bends (p = 0.6) shown in Fig. 3(c), higher $\kappa_0/2\pi$ with longer wavelength is observed, as well as spectrally periodic, vertical striations caused by inter-modal interference. Since the eigenmode mismatch between the straight waveguide and the circular bend is larger for longer wavelength, the spatial mode interaction is stronger and causes higher loss. These observations are further verified in the racetrack microresonator with circular bends (p = 0) shown in Fig. 3(e, f). Here, spatial mode interaction is so strong that many resonances experience greatly increased $\kappa_0/2\pi$, much higher than $\kappa_{ex}/2\pi$.

Single soliton generation and K-band phase noise characterization

Finally, we demonstrate single soliton generation of 19.8 GHz repetition rate in the racetrack microresonator with Euler bends. We observe a soliton step length of ~0.5 ms, on par with the previously reported value in a 100-GHz-FSR microresonator [10]. Due to the suppressed AMXs, the soliton step is sufficiently long, allowing for direct access to the single soliton state using simple laser piezo frequency tuning, without any other complex tuning schemes or auxiliary lasers. An erbium-doped fiber amplifier (EDFA) is used to increase the on-chip pump power to approximately 55.7 mW to seed soliton formation. Fig.4(a) shows the single soliton spectrum, which does not show prominent dispersive wave features caused by AMXs. The single soliton spectrum fit shows a 3-dB bandwidth of 16.3 nm, corresponding to a pulse duration of 156 fs.

Further single-sideband (SSB) phase noise measurement of the soliton repetition rate shows a weak quite point effect [11], indicating inhibited dispersive wave generation, due to suppressed spatial mode interaction and avoided-mode crossings.

Conclusion

In this work, we demonstrate a photonic design that suppresses spatial mode interaction and effectively operates multi-mode waveguides in the single-mode regime. Using a racetrack microresonator that features high-quality factor Q > 10^7 and consists of two straight waveguides and two adiabatic Euler bends, we quantitatively characterize the suppressed spatial mode interaction. The optimized Euler bends and racetrack microresonators can be building blocks for integrated nonlinear photonic systems, as well as linear circuits for programmable processors or photonic quantum computing.

Acknowledgements

This work was supported by the Air Force Office of Scientific Research (AFOSR) under Award No. FA9550-19-1-0250, by Contract HR0011- 20-2-0046 (NOVEL) from the Defense Advanced Research Projects Agency (DARPA), Microsystems Technology Office (MTO), by the Swiss National Science Foun- dation under grant agreement No. 176563 (BRIDGE), and by the EU H2020 research and innovation programme under grant agreement No. 965124 (FEMTOCHIP). The Si_3N_4 chips were fabricated in the EPFL center of MicroNanoTechnology (CMi).

References

[1] Herr, T., Brasch, V., Jost, J. D., Mirgorodskiy, I., Lihachev, G., Gorodetsky, M. L., & Kippenberg, T. J. (2014). “Mode spectrum and temporal soliton formation in optical microresonators”. *Physical review letters*, 113(12), 123901.
DOI: https://doi.org/10.1103/PhysRevLett.113.123901

[2] Ramelow, Sven, Alessandro Farsi, Stéphane Clemmen, Jacob S. Levy, Adrea R. Johnson, Yoshitomo Okawachi, Michael RE Lamont, Michal Lipson, and Alexander L. Gaeta. "Strong polarization mode coupling in microresonators." *Optics letters39,* no. 17 (2014): 5134-5137.
DOI: https://doi.org/10.1364/OL.39.005134

[3] Liu, Junqiu, Erwan Lucas, Arslan S. Raja, Jijun He, Johann Riemensberger, Rui Ning Wang, Maxim Karpov, Hairun Guo, Romain Bouchand, and Tobias J. Kippenberg. "Photonic microwave generation in the X- and K-band using integrated soliton microcombs." *Nature Photonics* 14, no. 8 (2020): 486-491.
DOI: https://doi.org/10.1038/s41566-020-0617-x

[4] Liu, Junqiu, Hao Tian, Erwan Lucas, Arslan S. Raja, Grigory Lihachev, Rui Ning Wang, Jijun He et al. "Monolithic piezoelectric control of soliton microcombs." *Nature* 583, no. 7816 (2020): 385-390.
DOI: https://doi.org/10.1038/s41586-020-2465-8

[5] Kordts, Arne, Martin HP Pfeiffer, Hairun Guo, Victor Brasch, and Tobias J. Kippenberg. "Higher order mode suppression in high-Q anomalous dispersion SiN microresonators for temporal dissipative Kerr soliton formation." *Optics letters* 41, no. 3 (2016): 452-455.
DOI: https://doi.org/10.1364/OL.41.000452

[6] Fujisawa, Takeshi, Shuntaro Makino, Takanori Sato, and Kunimasa Saitoh. "Low-loss, compact, and fabrication-tolerant Si-wire 90 waveguide bend using clothoid and normal curves for large scale photonic integrated circuits." *Optics express* 25, no. 8 (2017): 9150-9159.
DOI: https://doi.org/10.1364/OE.25.009150

[7] Vogelbacher, Florian, Stefan Nevlacsil, Martin Sagmeister, Jochen Kraft, Karl Unterrainer, and Rainer Hainberger. "Analysis of silicon nitride partial Euler waveguide bends." *Optics express* 27, no. 22 (2019): 31394-31406.
DOI: https://doi.org/10.1364/OE.27.031394

[8] Liu, Junqiu, Guanhao Huang, Rui Ning Wang, Jijun He, Arslan S. Raja, Tianyi Liu, Nils J. Engelsen, and Tobias J. Kippenberg. "High-yield, wafer-scale fabrication of ultralow-loss, dispersion-engineered silicon nitride photonic circuits." *Nature communications* 12, no. 1 (2021): 1-9.
DOI: https://doi.org/10.1038/s41467-021-21973-z

[9] Liu, Junqiu, Victor Brasch, Martin HP Pfeiffer, Arne Kordts, Ayman N. Kamel, Hairun Guo, Michael Geiselmann, and Tobias J. Kippenberg. "Frequency-comb-assisted broadband precision spectroscopy with cascaded diode lasers." *Optics Letters* 41, no. 13 (2016): 3134-3137.
DOI: https://doi.org/10.1364/OL.41.003134

[10] Liu, Junqiu, Arslan S. Raja, Maxim Karpov, Bahareh Ghadiani, Martin HP Pfeiffer, Botao Du, Nils J. Engelsen, Hairun Guo, Michael Zervas, and Tobias J. Kippenberg. "Ultralow-power chip-based soliton microcombs for photonic integration." *Optica* 5, no. 10 (2018): 1347-1353.
DOI: https://doi.org/10.1364/OPTICA.5.001347

[11] Yi, Xu, Qi-Fan Yang, Xueyue Zhang, Ki Youl Yang, Xinbai Li, and Kerry Vahala. "Single-mode dispersive waves and soliton microcomb dynamics." *Nature communications* 8, no. 1 (2017): 1-9.
DOI: https://doi.org/10.1038/ncomms14869